The superionic phase transition in hydrogen-bonded systems of the $M_3H(XO_4)_2$ class: the effect of nearest-O(2) distortions on the proton dynamics

2001 J. Phys.: Condens. Matter 13 4081

(http://iopscience.iop.org/0953-8984/13/18/316)

INSTITUTE OF PHYSICS PUBLISHING JOURNAL OF PHYSICS: CONDENSED MATTER

J. Phys.: Condens. Matter **13** (2001) 4081–4095 www.iop.org/Journals/cm PII: S0953-8984(01)22606-X

The superionic phase transition in hydrogen-bonded systems of the $M_3H(XO_4)_2$ class: the effect of nearest-O(2) distortions on the proton dynamics

Natalie I Pavlenko[1] **and Ihor Stasyuk**

Institute for Condensed Matter Physics, 1 Svientsitsky Street, UA-79011, Lviv, Ukraine

E-mail: natalie@icmp.lviv.ua (N I Pavlenko)

Received 7 March 2001

Abstract

We study the behaviour of protonic conductivity at the transition between the superionic state with a disordered system of hydrogen bonds and low-temperature states at which the different types of ordering in the H-bond network appear (as an example, the $M_3H(XO_4)_2$ class of crystals is considered). We apply a lattice-gas-type model incorporating the two-stage Grotthuss mechanism for proton transport and the interaction between the protons and distortions of nearest oxygen ions causing a strong quasi-polaron effect. The temperature dependences of the conductivity and its reorientational inter-bond and intra-bond contributions are analysed and compared with experimental measurements as well as with the results obtained on the basis of a simplified one-minimum approximation for the H-bond potential. Detailed analysis of the activation energies in the low- and high-temperature phases allows us to infer a more complex character of the superionic transition, suggesting that a possible intermediate transition from the state with more strongly localized protons to the weaker proton-localized state occurred on heating between the ordered and superionic phases.

1. Introduction

It is observed that the proton dynamics in hydrogen-bonded superprotonic crystals changes drastically at the transitions from superionic phases with the disordered structure of the H-bond network to the low-temperature phases with the frozen-in sublattice of hydrogen bonds. The fast proton transport in the superionic state is achieved mainly due to the thermally activated hopping with low activation energy ($\sim$0.1 eV), whereas below the superionic transition temperature the environment containing the H-bonded anionic groups strongly influences the proton dynamics, resulting in the stronger localization of protons residing on the H bonds and

[1] Present address: Institut für Physikalische Chemie und Elektrochemie, Universität Hannover, Callinstrasse 3-3a, D-30167, Hannover, Germany.

0953-8984/01/184081+15$30.00

a drop in the proton conductivity. It is generally accepted from the results of neutron scattering studies [1, 2] that the proton transport proceeds in the framework of the two-stage Grotthuss mechanism involving the transfer of the proton within the H bond (intra-bond motion) and breaking of the H bond together with the reorientation of the ionic group involved in the H-bond formation (inter-bond transfer). Despite the detailed experimental investigations of the proton migration process, there still exist unresolved problems in the theoretical modelling of this phenomenon. Firstly, such a model must describe accurately the coupling with lattice distortions which could lead to non-trivial dynamics of protons in the H-bonded network as has been shown in [3, 4]. Secondly, the above-mentioned two elementary stages of the transport mechanism must be incorporated into the model to take account of the complex interplay between inter-bond and intra-bond hopping.

In this work we choose the crystals of the $M_3H(XO_4)_2$ (M = Rb, Cs, NH_4; X = Se, S) family as the objects for investigation. The reason is that in these compounds the conductivity is significantly higher in the conducting planes (001) formed by the vertex O(2) oxygens connected by the virtual H bonds in superionic phases. Thus, we can focus on the analysis of proton mobility in quasi-two-dimensional systems. The basic crystal structure in the superionic phase with the lattice vectors

$$\boldsymbol{a}_1 = \left(-\frac{\sqrt{3}}{2}a_0, \frac{1}{2}a_0, \frac{1}{3}c\right) \qquad \boldsymbol{a}_2 = \left(\frac{\sqrt{3}}{2}a_0, \frac{1}{2}a_0, \frac{1}{3}c\right) \qquad \boldsymbol{a}_3 = \left(0, -a_0, \frac{1}{3}c\right)$$

($a_0 = 3.5$ Å, $c = 22.9$ Å) is shown in figure 1(a). There are two XO_4 groups and three virtual (possible) hydrogen bonds $f = 1, 2, 3$ adjacent to the upper group ($XO_4^{(1)}$) in the unit cell with coordinate $\boldsymbol{R}_m = m_1\boldsymbol{a}_1 + m_2\boldsymbol{a}_2 + m_3\boldsymbol{a}_3$. Another three hydrogen bonds near the lower ($XO_4^{(2)}$) group belong to the neighbouring unit cells with the vectors $\boldsymbol{R}_m - \boldsymbol{a}_f$. The proton transport in the (001) planes is sustained due to the dynamical formation and breaking of the virtual hydrogen bonds between the O(2)-oxygen ions with a one-third probability of each hydrogen bond existing. Figure 1(b) represents a typical scheme of proton migration within the conducting plane with the arrows indicating one of the possible paths for the proton. We introduce here the transfer parameters Ω_T and Ω_R to describe respectively the intra-bond and inter-bond stages of the transport mechanism. The two different types of ordered H-bond network usually observed in these systems on cooling are described in more detail in [5, 6]. We note here that whereas the first case is distinguished by parallel sequences of H-bonded dimers, doubling of the unit cell along one of the translation vectors $\boldsymbol{a}_f$ occurs with the second type of ordering (for instance, the H-bond network consists of dimeric sequences along $\boldsymbol{a}_1$- and $\boldsymbol{a}_2$-directions changing alternately with the translation along $\boldsymbol{a}_3$, which corresponds to the ordering with the $\boldsymbol{k}_4 = \frac{1}{2}\boldsymbol{b}_3$ vector).

The above-described rearrangements of the H-bond network at the transition from the superionic phase have been studied in the framework of the lattice-gas-type model [7, 8] with the following Hamiltonian:

$$H_p = \frac{1}{2}\sum_{\substack{mm'\\ ff'}} \Phi_{ff'}(mm')n_{mf}n_{m'f'} - \mu\sum_{mf} n_{mf} \tag{1}$$

where $n_{mf} = \{0, 1\}$ is the proton occupation number for the fth H bond; $\Phi_{ff'}(mm')$ is the energy of the proton interactions; μ denotes the chemical potential which has to be found for the given average proton concentration.

The effect of the environment is of crucial importance for the proton subsystem properties of these compounds as well as other proton conductors [5, 9]. In particular, it is shown in [3] that the coupling with the dynamics of the XO_4 tetrahedra can give rise to instability in

the system and formation of the dimerized H-bonded structure with the frozen-in tetrahedra distortions which is observed in the compounds of this family. On the other hand, the impact of the coupling of protons with optical vibration phonon modes on the proton mobility has been studied theoretically in [6]. However, in this case the process of proton transport was considered as induced by the reorientational tetrahedra dynamical hopping of the protonic quasi-polarons between the virtual H bonds with effective transfer parameter Ω_R, assuming the single-well approximation for the H-bond potential. As distinct from the previous approach [6], in this work the mechanism of the proton transport is described in the framework of the generalized two-stage model which incorporates the process of proton transfer within H bonds and takes into account the change of the proton transfer integral with the shortening distance between H-bonded ionic groups. We estimate the contributions of reorientational and intra-bond hopping terms to the activation energy for proton migration and to the total conductivity coefficient σ. Furthermore, we compare the temperature behaviour of σ for $(NH_4)_3H(SeO_4)_2$ (TAHSe) in the vicinity of the superionic transition obtained within our two-stage approach with the results from the one-minimum approximation [6] and with experimental values given in [10]. The comparison with experiment in the temperature interval $T < T_{si}$ (T_{si} is the superionic transition temperature) makes it necessary for us to suggest a significant change of the energy of binding of the protonic quasi-polaron (formed due to the coupling with O(2) distortions) with the superionic transition. This change caused by the modification of effective proton–oxygen distortion interactions induces an additional drastic increase of the activation energy in the low-temperature ordered phases and is possibly the reason for the precursor effect observed recently at $\sim$1.5 K below T_{si} in the latest calorimetric studies of $M_3H(XO_4)_2$ reported in [11].

2. Description of the proton-transport mechanism

The disordered proton subsystem strongly affects the sublattice of ionic groups leading to rather unusual dynamical behaviour of H-bonded XO_4 tetrahedra. Besides the fast rotational motion of XO_4 in superionic phases causing a breaking of H bonds which are weaker (longer) in superionic states, the appearance of a mobile proton between nearest XO_4 tetrahedra induces distortions of the nearest O(2) oxygens towards the proton (figure 1(c)). As long as the proton is redistributed between three possible positions (virtual bonds) in the unit cell, the O(2) oxygens affected by the proton inter-bond hopping can be displaced towards one of the three distorted positions as well [12], as is indicated in figure 1(c) by arrows. This important aspect of proton–oxygen coupling observed in x-ray scattering experiments [13–15] reinforces the necessity of incorporating the interactions with the distortions of oxygen ions into the model. Firstly, analogously to the simpler approach described in [6], we account for the modification of the H-bond potential due to above-described anti-phase optical vibration modes of the O(2) sublattice. The corresponding analytical terms are derived in detail in [6] and we present here the final expressions in the second-quantization form:

$$H^1_{pr-ph} = \sum_{mf} \sum_{qj} \tau_{mf}(\boldsymbol{q}j)(b_{qj} + b^+_{-qj})n_{mf} \tag{2}$$

where b^+_{qj}, b_{qj} are the phonon creation and annihilation operators of the jth optical branch for the vector $\boldsymbol{q}$. The coefficients $\tau_{mf}(\boldsymbol{q}j)$ are given by

$$\tau_{mf}(\boldsymbol{q}j) = \sqrt{\frac{\hbar}{2NM\omega_j(\boldsymbol{q})}}\, \nabla V \exp[\mathrm{i}\boldsymbol{q}\cdot\boldsymbol{R}_m] \sum_{\alpha=x,y} \beta_\alpha (u_{j\alpha}(1) + u_{j\alpha}(2)\exp[\mathrm{i}\boldsymbol{q}\cdot\boldsymbol{a}_f]) \tag{3}$$

where

$$\beta_x = (-1, 1, 0) \qquad \beta_y = \frac{1}{\sqrt{3}}(1, -1, -2)$$

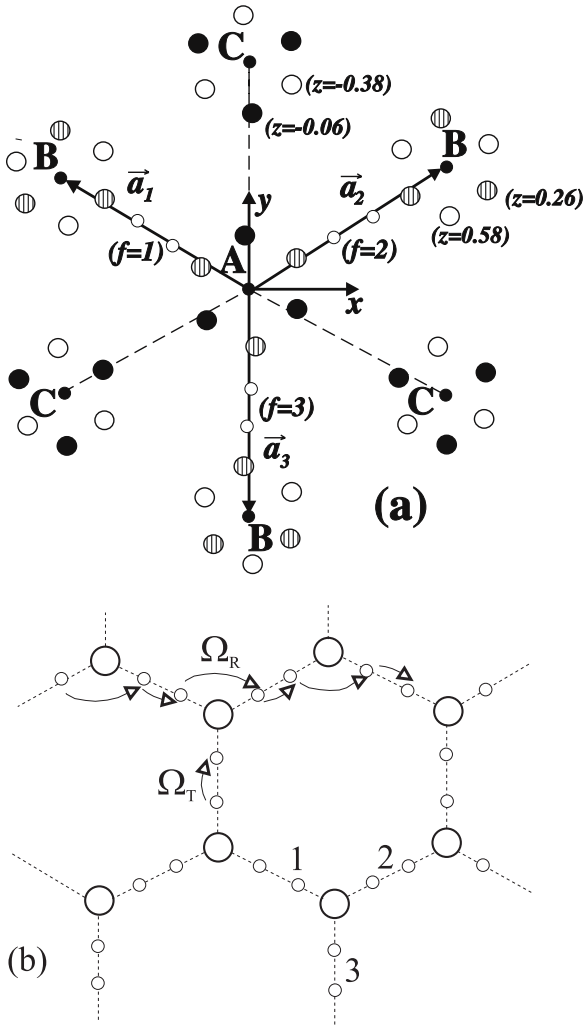

Figure 1. (a) The projection of the rhombohedral primitive unit cell of $M_3H(XO_4)_2$ with lattice vectors $\boldsymbol{a}_1$, $\boldsymbol{a}_2$, $\boldsymbol{a}_3$ on the (001) plane in the hexagonal coordinate system in the superionic phase. The open, solid and hatched big circles correspond to the possible positions of O(2) oxygens with the different values of z; A ($z = 0$), B ($z = 1/3$) and C ($z = -1/3$) denote the positions of X atoms in $XO_4^{(2)}$ groups. The small circles indicate the proton positions within the hydrogen bond. (b) The H-bond network in the (001) plane in the disordered superionic phase with average occupancies of each virtual bond (m, f) (indicated by dashed line) $\bar{n}_{mf} = 1/3$. (c) A schematic representation of the distortions (shown by arrows) of the nearest oxygen ions O(2) from the central positions (the three possible distorted positions for each O(2) are indicated by large circles) towards the proton located between them.

where ∇V is the change of the proton potential with the change of the inter-oxygen distance, M is the oxygen ion mass; $\omega_j(\boldsymbol{q})$ are the phonon frequencies and the $u_{j\alpha}(l)$ given by

$$\boldsymbol{u}_1(1;2) = [0,-1;0,1] \qquad \boldsymbol{u}_2(1;2) = [-1,0;1,0]$$

($j = 1, 2$ denotes the jth anti-phase vibration branch and the index $l = 1, 2$ corresponds to the upper and lower sublattices of $O(2)^{(l)}$ oxygens) are the polarization vectors of the O(2)-oxygen subsystem. The vibration energy of the O(2) oxygens in the harmonic approximation

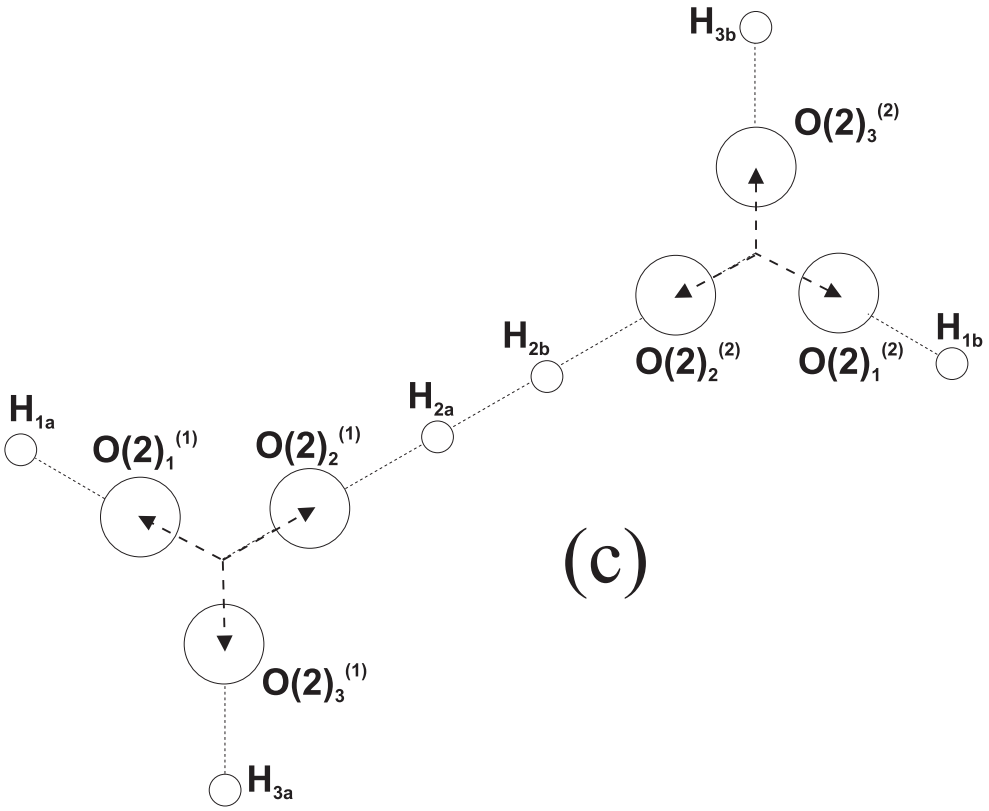

Figure 1. (Continued)

is given by

$$H_{ph} = \sum_{qj} \hbar\omega_j(\boldsymbol{q}) b^+_{qj} b_{qj}. \tag{4}$$

We turn now to the two-stage process of proton migration. To describe various proton configurations in the double-well H-bond potential, the following states for a proton on each (m, f) bond are introduced:

$$|0\rangle_{mf} = |00\rangle_{mf} \qquad |a\rangle_{mf} = |10\rangle_{mf} \qquad |b\rangle_{mf} = |01\rangle_{mf}. \tag{5}$$

The first state corresponds to the absence of H bonds (no protons between the nearest vertex oxygens) and the two other states $|a\rangle_{mf}$ and $|b\rangle_{mf}$ describe one proton in the left or right well on the bond. We eliminate the state $|11\rangle_{mf}$ with two protons between ionic groups (the Bjerrum D defect) assuming extremely strong repulsion between the protons in this state. On introducing the Hubbard operators $X^{pr}_{mf} = |p\rangle_{mf}\langle r|_{mf}$, the quantum tunnelling within the H bond with the tunnelling integral Ω_T can be represented by the following term:

$$H_T = \Omega_T \sum_{mf} (X^{ab}_{mf} + X^{ba}_{mf}) \tag{6}$$

whereas the reorientation inter-bond hopping term [6] takes here the form

$$H_R = \Omega_R \sum_{\substack{f \\ f \neq f'}} (X^{a0}_{mf} X^{0a}_{mf'} + X^{b0}_{mf} X^{0b}_{m+\boldsymbol{a}_f - \boldsymbol{a}_{f'}, f'}) \tag{7}$$

with the inter-bond transfer integral Ω_R. The operators of proton occupancy for the H bond can be expressed in terms of the Hubbard operators as $n_{mf} = X^{aa}_{mf} + X^{bb}_{mf}$. In addition to (2), we take into account the modification of the intra-bond tunnelling integral due to the coupling with the vertex oxygen vibrations:

$$H^2_{pr-ph} = \sum_{mf} \sum_{\substack{q \\ j=2,4}} \rho_{mf}(\boldsymbol{q}j)(b_{\boldsymbol{q}j} + b^+_{-\boldsymbol{q}j})(X^{ab}_{mf} + X^{ba}_{mf}). \tag{8}$$

The coefficients $\rho_{mf}(\boldsymbol{q}j)$ have a form similar to (3), by geometric reasoning, with the substitution of $\nabla\Omega_T$ in place of ∇V, where the parameter $\nabla\Omega_T$ characterizes the modification of Ω_T with the change of the distance between H-bonded oxygens.

Applying the unitary Lang–Firsov transformation,

$$\begin{aligned}
&\tilde{H} = \exp(\mathrm{i}S)H\exp(-\mathrm{i}S) \\
&S = \sum_{\substack{mf \\ s=a,b}} v_{mfs}\tilde{X}^{ss}_{mf} \qquad\qquad v_{mfs} = \mathrm{i}\sum_{qj} \frac{\tau^s_{mf}(\boldsymbol{q}j)}{\hbar\omega_j(\boldsymbol{q})}(b_{\boldsymbol{q}j} - b^+_{-\boldsymbol{q}j}) \\
&\tau^{a/b}_{mf}(\boldsymbol{q}j) = \tau_{mf}(\boldsymbol{q}j) \pm \rho_{mf}(\boldsymbol{q}j) \qquad \tilde{X}^{ss}_{mf} = \frac{1}{2}(X^{aa}_{mf} + X^{bb}_{mf} \pm (X^{ab}_{mf} + X^{ba}_{mf}))
\end{aligned} \tag{9}$$

where H is given by the expressions (1)–(8), allows us to diagonalize the terms (6) and (8) and consider the new equilibrated states of relaxed O(2) oxygens with protonic quasi-polarons formed due to the coupling (2) and (8). We present below the Hamiltonian (9) with inter-proton interactions taken in the mean-field approximation:

$$\tilde{H} = \sum_{mf}\{(\Omega_T - \mu)\tilde{X}^{aa}_{mf} - (\Omega_T + \mu)\tilde{X}^{bb}_{mf}\} + \sum_{mfs}\gamma_{fs}(m)\tilde{X}^{ss}_{mf} + \sum_{qj}\hbar\omega_j(\boldsymbol{q})b^+_{qj}b_{qj} + \tilde{H}_R + U_0 \tag{10}$$

where $\gamma_{fs}(m) = \gamma_f(m) - \delta^s_{mf} - \Delta^s_{mf}$ is the internal field

$$\gamma_f(m) = \sum_{m'f'}\Phi_{ff'}(mm')\langle n_{m'f'}\rangle$$

renormalized by the coupling with oxygen distortions:

$$\delta^s_{mf} = \sum_{m'f's'}\sum_{qj}\frac{\tau^s_{mf}(\boldsymbol{q}j)\tau^{s'}_{m'f'}(-\boldsymbol{q}j)}{\hbar\omega_j(\boldsymbol{q})}\langle\tilde{X}^{s's'}_{m'f'}\rangle \qquad \Delta^s_{mf} = \sum_{qj}\frac{|\tau^s_{mf}(\boldsymbol{q}j)|^2}{\hbar\omega_j(\boldsymbol{q})}$$

$$U_0 = -\frac{1}{2}\sum_{\substack{mf \\ m'f'}}\Phi_{ff'}(mm')\langle n_{mf}\rangle\langle n_{m'f'}\rangle + \sum_{\substack{mfs \\ m'f's'}}\sum_{qj}\frac{\tau^s_{mf}(\boldsymbol{q}j)\tau^{s'}_{m'f'}(-\boldsymbol{q}j)}{\hbar\omega_j(\boldsymbol{q})}\langle\tilde{X}^{ss}_{mf}\rangle\langle\tilde{X}^{s's'}_{m'f'}\rangle$$

with $\langle\tilde{X}^{ss}_{mf}\rangle$ denoting the average occupancy of the proton state $|\tilde{s}\rangle_{mf}$ $(s = a, b)$. The part (7) describing the rotational hopping after the transformation (9) takes the form

$$\begin{aligned}
\tilde{H}_R = \frac{\Omega_R}{2}\sum_{\substack{m \\ f\neq f'}}\sum_{ss'}\{&(-1)^{\delta_{ss'}+1}\tilde{X}^{s0}_{mf}\tilde{X}^{0s'}_{mf'}Z^{ss'}_{ff'}(mm) \\
&+ \tilde{X}^{s0}_{mf}\tilde{X}^{0s'}_{m+\boldsymbol{a}_f-\boldsymbol{a}_{f'},f'}Z^{ss'}_{ff'}(m, m+\boldsymbol{a}_f-\boldsymbol{a}_{f'})\}
\end{aligned}$$

where the operators

$$\begin{aligned}
&Z^{ss'}_{ff'}(mm') = \exp\left\{-\sum_{qj}\frac{\Delta\tau^{ss'}_{ff'}(\boldsymbol{q}j|mm')(b_{\boldsymbol{q}j} - b^+_{-\boldsymbol{q}j})}{\hbar\omega_j(\boldsymbol{q})}\right\} \\
&\Delta\tau^{ss'}_{ff'}(\boldsymbol{q}j|mm') = \tau^s_{mf}(\boldsymbol{q}j) - \tau^{s'}_{m'f'}(\boldsymbol{q}j)
\end{aligned} \tag{11}$$

specify the band-narrowing factors generalized by introducing here double-well proton states.

In order to analyse the protonic conductivity in the framework of Kubo theory [16], we should evaluate the expression for the correlation function $\langle J(z)J(0)\rangle$ where z is the time argument. The proton current operator

$$J = \frac{e}{\mathrm{i}\hbar}[H, x]$$

(where

$$x = \sum_{mfs} X^{ss}_{mf} \boldsymbol{R}^{s}_{mf}$$

is the proton polarization operator, $\boldsymbol{R}^{s}_{mf}$ $(s = a, b)$ are the proton coordinates in the double-well H bond) after transformation (9) consists of two parts: $\tilde{J} = \tilde{J}_T + \tilde{J}_R$. The first term

$$\tilde{J}_T = \frac{e}{\mathrm{i}\hbar}\sum_{mf} \boldsymbol{R}^{ab}_{f}\Bigg(\Omega_{mf}\bar{Z}^{ba}_{ff}(mm) + \frac{1}{2}\sum_{qj}\rho_{mf}(\boldsymbol{q}j)[B_{qj}\bar{Z}^{ba}_{ff}(mm) + \bar{Z}^{ba}_{ff}(mm)B_{qj}]\Bigg)\tilde{X}^{ba}_{mf} + \mathrm{H.c.} \tag{12}$$

describes the intra-bond transfer processes assisted by the oxygen dynamics. Here

$$\boldsymbol{R}^{ab}_{f} = \boldsymbol{R}^{a}_{mf} - \boldsymbol{R}^{b}_{mf} \qquad B_{qj} = b_{qj} + b^{+}_{-qj}$$

and

$$\Omega_{mf} = \Omega_T + 2\sum_{m'f's'}\sum_{qj}\frac{\tau^{s's'}_{m'f'}(-\boldsymbol{q}j)}{\hbar\omega_j(\boldsymbol{q})}\rho_{mf}(\boldsymbol{q}j)\langle\tilde{X}^{s's'}_{m'f'}\rangle + 2\sum_{qj}\frac{\rho_{mf}(\boldsymbol{q}j)\tau_{mf}(-\boldsymbol{q}j)}{\hbar\omega_j(\boldsymbol{q})}.$$

The rotation part of the current operator is given by

$$\tilde{J}_R = -\frac{e}{i\hbar}\frac{\Omega_R}{2}\sum_{\substack{m\\ f\neq f'}}\sum_{ss'}\boldsymbol{R}_{ff'}\big((-1)^{\delta_{ss'}+1}\tilde{X}^{s0}_{mf}\tilde{X}^{0s'}_{mf'}\bar{Z}^{ss'}_{ff'}(mm) - \tilde{X}^{s0}_{mf}\tilde{X}^{0s'}_{m+\boldsymbol{a}_f-\boldsymbol{a}_{f'},f'}\bar{Z}^{ss'}_{ff'}(m, m+\boldsymbol{a}_f-\boldsymbol{a}_{f'})\big) \tag{13}$$

where

$$\boldsymbol{R}_{ff'} = \boldsymbol{R}^{a}_{mf} - \boldsymbol{R}^{a}_{mf'} = -(\boldsymbol{R}^{b}_{mf} - \boldsymbol{R}^{b}_{m+\boldsymbol{a}_f-\boldsymbol{a}_{f'},f'})$$
$$\bar{Z}^{ss'}_{ff'}(m, m') = Z^{ss'}_{ff'}(m, m') - \langle Z^{ss'}_{ff'}(m, m')\rangle.$$

The resulting conductivity coefficient can be written as $\sigma(\omega) = \sigma_T + \sigma_R + \sigma_{TR}$, where σ_T is the contribution from the intra-bond transfer processes, σ_R corresponds to the reorientational phonon-assisted hopping and σ_{TR} describes the mixed intra-bond + reorientation dynamics.

First we focus on the essentially new intra-bond contribution to σ arising from the thermally activated proton hopping in a double-well potential. To derive the expression for σ_T in the second-order perturbation theory with respect to Ω_R, we assume the existence of a regime of strong proton–phonon coupling for our system when the following condition is valid:

$$\sum_{qj}\frac{|\Delta\tau^{ss'}_{ff'}(mm'|\boldsymbol{q}j)|^2}{(\hbar\omega_j(\boldsymbol{q}))^2\sinh\frac{1}{2}\beta\hbar\omega_j(\boldsymbol{q})} \gg 1.$$

Using the method of steepest descent to perform the time integration [17], we obtain the following expressions for σ_T along the direction given by the vector $\boldsymbol{r}$:

$$\sigma^{r}_{T}(\omega, T) = \frac{e^2}{\hbar^2}\frac{\sqrt{\pi}}{v_c}\tilde{\tau}^{ab}_{T}\mathrm{e}^{-\beta E^{ab}_{T}/3}\frac{\sinh\beta\hbar\omega/2}{\hbar\omega/2}\sum_{f}(\boldsymbol{R}^{ab}_{f}(\boldsymbol{r}))^2(s^{(1)}_{f}\langle\tilde{X}^{bb}_{mf}\rangle + s^{(2)}_{f}\langle\tilde{X}^{aa}_{mf}\rangle) \tag{14}$$

where $\boldsymbol{R}_f^{ab}(\boldsymbol{r})$ is the projection of $\boldsymbol{R}_f^{ab}$ on $\boldsymbol{r}$ and the weight factors are given by

$$s_f^{(j)} = \left[\Omega_f^2 - \frac{2}{9}\bar{n}_0(1+\bar{n}_0)(E_T^{ab})^2\right]c_{f,0}^{(j)} + \frac{1}{9}(E_T^{ab})^2\left((1+\bar{n}_0)^2 c_{f,-2}^{(j)} + \bar{n}_0^2 c_{f,2}^{(j)}\right) + \frac{1}{3}E_T^{ab}\left[\left(\pm 2\Omega_f + \frac{1}{2}\hbar\omega_0\right)(1+\bar{n}_0)c_{f,-1}^{(j)} + \left(\mp 2\Omega_f + \frac{1}{2}\hbar\omega_0\right)\bar{n}_0 c_{f,1}^{(j)}\right]. \quad (15)$$

The coefficients

$$c_{f,l}^{(1/2)} = \exp(\pm\frac{1}{2}\beta\hbar\Omega_{f,l} - (\tilde{\tau}_T^{ab})^2(\omega \pm \Omega_{f,l})^2)$$

($\hbar\Omega_{f,l} = -2\Omega_T + \gamma_{fb} - \gamma_{fa} + l\hbar\omega_0$) and $\bar{n}_0$ is the average number of phonons with the energy $\hbar\omega_0$ determined by the Bose distribution. The polaron binding energy

$$E_T^{ab} = \frac{(\hbar\nabla v_{ab})^2}{2M(\hbar\omega_0)^2}$$

($\nabla v_{ab} = \nabla v_a - \nabla v_b = 2\nabla\Omega_T$, $\nabla v_{a/b} = \nabla V \pm \nabla\Omega_T$ with $\omega_j(\boldsymbol{q}) = \omega_0$ taken in the dispersionless approximation) is required to provide a hopping of the protonic polaron between two localized positions within the H bond, and the parameter $\tilde{\tau}_T^{ab}$ which is given by

$$\frac{1}{(\tilde{\tau}_T^{ab})^2} = 2\sum_{\boldsymbol{q}j}\frac{|\Delta\tau_{ff}^{ab}(mm|\boldsymbol{q}j)|^2}{\hbar^2\sinh\frac{1}{2}\beta\hbar\omega_j(\boldsymbol{q})} \qquad (\tilde{\tau}_T^{ab})^2 = \frac{3}{16}\beta\frac{\hbar^2}{E_T^{ab}} \quad (16)$$

characterizes the average hopping time length between two localized positions within the H bond.

To evaluate the correlation functions $\langle\tilde{J}_R(z)\tilde{J}_R\rangle$ we apply the following decoupling procedure for the proton part given by Hubbard operators:

$$\langle\tilde{X}_{kf'}^{s0}(z)\tilde{X}_{k'f}^{s'0}(z)\tilde{X}_{k_1f}^{s'0}\tilde{X}_{k_1',f'}^{0s}\rangle \to \delta_{k,k_1'}\delta_{k'k_1}\langle\tilde{X}_{kf'}^{s0}(z)\tilde{X}_{kf'}^{0s}\rangle\langle\tilde{X}_{k'f}^{0s'}(z)\tilde{X}_{k'f}^{s'0}\rangle \quad (17)$$

in the reciprocal-space representation:

$$\tilde{X}_{mf}^{s0} = \frac{1}{\sqrt{N/2}}\sum_{\boldsymbol{k}}\tilde{X}_{kf}^{s0}\mathrm{e}^{\mathrm{i}\boldsymbol{k}\cdot\boldsymbol{R}_m}.$$

Using the inter-bond current part (13) and approximation (17), we have the following expression for inter-bond contribution:

$$\sigma_R^r = \frac{e^2}{\hbar^2}\frac{\sqrt{\pi}}{v_c}\frac{\Omega_R}{2N^2}\sum_{f\neq f'}(\boldsymbol{R}_{ff'}^r)^2\int_0^\infty \mathrm{d}t\ \mathrm{e}^{\mathrm{i}(\omega+\mathrm{i}\varepsilon)t} \times \int_0^\beta \mathrm{d}\lambda\sum_{\boldsymbol{k},\boldsymbol{k}_1}\left\{\sum_{ss'}P^{ss'}\mathrm{e}^{-(z+\frac{1}{2}i\hbar\beta)^2/4(\tilde{\tau}_R^{ss'})^2}\langle\tilde{X}_{\boldsymbol{k},f}^{s0}(z)\tilde{X}_{\boldsymbol{k},f}^{0s}\rangle\langle\tilde{X}_{\boldsymbol{k}_1,f'}^{0s'}(z)\tilde{X}_{\boldsymbol{k}_1,f'}^{s'0}\rangle\right\} \quad (18)$$

with $z = t - \mathrm{i}\hbar\lambda$, $P^{ss} = \mathrm{e}^{-5\beta E_R^s/6}$ and $P^{ab} = \mathrm{e}^{-\beta E_R^{ab}/3}$. In contrast to the simple one-well approach [6], we have in (18) instead of the one-polaron dissociation energy $E_0 = (\hbar\nabla V)^2/2M(\hbar\omega_0)^2$ three different $E_R^{ss'}$ given by

$$E_R^s = \frac{(\hbar\nabla v_s)^2}{2M(\hbar\omega_0)^2} \qquad E_R^{ab} = \frac{\hbar^2[(\nabla v_a)^2 + (\nabla v_b)^2 + \nabla v_a\nabla v_b/2]}{2M(\hbar\omega_0)^2}. \quad (19)$$

Consequently, instead of only one effective time parameter $\tilde{\tau}$ ($\tilde{\tau}^2 = \frac{3}{40}\beta\hbar^2/E_0$) we have three different parameters $\tilde{\tau}_R^s$ and $\tilde{\tau}_R^{ab}$:

$$(\tilde{\tau}_R^{ss})^2 = \frac{3}{40}\beta\hbar^2/E_R^s \qquad (\tilde{\tau}_R^{ab})^2 = \frac{3}{16}\beta\hbar^2/E_R^{ab} \quad (20)$$

characterizing the average time length of the proton inter-bond hopping between the states $|\tilde{s}\rangle_f \to |\tilde{s}\rangle_{f'}$ ($s = a, b$) and $|\tilde{a}\rangle_f \to |\tilde{b}\rangle_{f'}$, $|\tilde{b}\rangle_f \to |\tilde{a}\rangle_{f'}$. It is worth noting that the relation $\tilde{\tau}_T^{ab} > \{\tilde{\tau}_R^{ab}, \tilde{\tau}_R^s\}$ follows from (16) and (20) ($\tilde{\tau}_R^{ss'}/\tilde{\tau}_T^{ab} \sim 0.1$), i.e. the rate of proton transfer within the H bond is lower than that of the rotational hopping. This is in agreement with the results of the modelling by MD simulations in [18] as well as with experimental data [1]. We use, analogously to the intra-bond case, the steepest-descent approach for time integration in (18). Furthermore, the analysis of the term σ_{TR} shows that the latter is negligibly small at temperatures in the vicinity of the superionic phase transition in comparison with (14) and (18) for the strong-proton–phonon-coupling regime due to the presence of additional prefactors like

$$P_2^s = \exp\left(-\frac{E_R^s}{\beta(\hbar\omega_0)^2}(\alpha\cosh\beta\hbar\omega_0/2 - 1)\right)$$

($\alpha = \text{constant} > 0$).

Next we determine the averages $\langle\tilde{X}^{s0}_{\boldsymbol{k},f}(z)\tilde{X}^{0s'}_{\boldsymbol{k},f'}\rangle$ and

$$\langle\tilde{X}^{ss'}_{mf}\rangle = \frac{2}{N}\sum_{\boldsymbol{k}}\langle\tilde{X}^{s0}_{kf}\tilde{X}^{0s'}_{kf}\rangle$$

appearing in (14) and (18) using the spectral theorem which allows one to express these quantities in terms of the corresponding Green functions

$$G^{ss'}_{ff'}(ii'|\boldsymbol{k}) = \langle\langle\tilde{X}^{0s}_{\boldsymbol{k}f}|\tilde{X}^{s'0}_{\boldsymbol{k}f'}\rangle\rangle_\omega.$$

To develop the equations of motion for $G^{ss'}_{ff'}(ii'|\boldsymbol{k})$ (the labels $i = \{+, -\}$ correspond to even and odd indices m_3 of the mth unit cell respectively),

$$\begin{aligned}(\hbar\omega + \Omega_T(-1)^{\delta_{sa}} + \mu - \gamma^i_{fs})&G^{ss'}_{ff'}(ii'|\boldsymbol{k}) \\ &= (\langle\tilde{X}^{00}_{fi}\rangle + \langle\tilde{X}^{ss}_{fi}\rangle)\Bigg\{\delta^{ss'}_{ff'}(i - i') \\ &\quad + \frac{\Omega_R}{2}\sum_{f_1'\neq f}\sum_{s_1'}\langle Z^{ss_1'}_{ff_1'}\rangle\left[(-1)^{1+\delta_{s_1's'}}G^{s_1's'}_{f_1',f'}(ii'|\boldsymbol{k}) + \mathrm{e}^{-\mathrm{i}\boldsymbol{k}(\boldsymbol{a}_f - \boldsymbol{a}_{f_1'})}G^{s_1's'}_{f_1',f'}(i_1'i'|\boldsymbol{k})\right]\Bigg\}\end{aligned} \tag{21}$$

(here $\langle\tilde{X}^{00}_{fi}\rangle = 1 - \langle\tilde{X}^{aa}_{fi}\rangle - \langle\tilde{X}^{bb}_{fi}\rangle$ and the index: $i_1' = i$ if f and $f_1' \neq 3$; $i_1' = \bar{i}$ if f or $f_1' = 3$) we apply the Hubbard-I-type decoupling procedure:

$$\langle\langle\tilde{X}^{s_1s_2}_{m_1f_1}\tilde{X}^{0s}_{mf}|\tilde{X}^{s'0}_{m'f'}\rangle\rangle_\omega \to \langle\tilde{X}^{s_1s_2}_{m_1f_1}\rangle\langle\langle\tilde{X}^{0s}_{mf}|\tilde{X}^{s'0}_{m'f'}\rangle\rangle_\omega.$$

As the starting point in the solution of the system (21) by the iteration procedure, we take the averages $\langle\tilde{X}^{ss}_{fi}\rangle$ determined from $\langle n_{fi}\rangle$ with the system Hamiltonian (10). In this case, for the description of the different types of proton ordering occurring in $M_3H(XO_4)_2$ we introduce the order parameters [7]. Specifically, to describe the transition from the superionic disordered phase to the orientation state characterized by the vector $\boldsymbol{k}_4 = \frac{1}{2}\boldsymbol{b}_3$ in phase III (TAHSe) and $\boldsymbol{k}_7 = 0$ (phase IV with parallel sequences of H-bonded dimers), we consider the two order parameters

$$u = \frac{1}{\sqrt{2}}(\langle n_{1+}\rangle - \langle n_{2+}\rangle) \qquad v = \frac{1}{\sqrt{6}}(\langle n_{1+}\rangle + \langle n_{2+}\rangle - 2\langle n_{3+}\rangle) \tag{22}$$

with the thermodynamical averages $\langle n_{1-}\rangle = \langle n_{2+}\rangle$, $\langle n_{2-}\rangle = \langle n_{1+}\rangle$ and $\langle n_{3-}\rangle = \langle n_{3+}\rangle$. Here the internal fields $\gamma_f(m)$ take the forms

$$\gamma_{1/2}(m) = \gamma_0 + av \pm b\mathrm{e}^{\mathrm{i}\boldsymbol{k}_4\cdot\boldsymbol{R}_m}u \qquad \gamma_3(m) = \gamma_0 - 2av$$

where

$$\gamma_0 = \frac{\bar{n}}{3}\sum_{f'}\Phi_{ff'}(0) \qquad a = \frac{1}{\sqrt{6}}[\Phi_{11}(0) - \Phi_{12}(0)] \qquad b = \frac{1}{\sqrt{2}}[\Phi_{11}(\boldsymbol{k}_4) - \Phi_{12}(\boldsymbol{k}_4)]$$

($\Phi_{ff'}(\boldsymbol{k})$ is the Fourier transform of the proton interaction potential $\Phi_{ff'}(mm')$).

To develop the expressions for the average proton occupancies $\langle n_{fi}\rangle$, we apply the high-density expansion method with additional inclusion of the Gaussian molecular-field fluctuations (GFA) [6]. This approach provides a significant decrease of the evaluated superionic transition temperature and makes possible a quantitative comparison between the results obtained theoretically and experimental data. For example, for $\tilde{b} = b/a = 1.688$ corresponding to TAHSe crystal [5], we have $T_c^{GFA} = 330$ K which agrees closely with the experimentally obtained value $T_c = 302$ K.

In this way, using the above-mentioned self-consistent procedure for the determination of $\langle \tilde{X}_{fi}^{ss}\rangle$ and $\langle \tilde{X}_{\boldsymbol{k},f}^{s0}(z)\tilde{X}_{\boldsymbol{k},f'}^{0s'}\rangle$ provides the possibility of evaluating the conductivity on the basis of expressions (14) and (18). We shall discuss later the consequences of the proton–phonon coupling effect, intra-bond proton transfer and the superionic phase transformations, focusing on the analysis of the conductivity coefficients obtained.

3. Discussion of the results

Since it is observed that the protonic conductivity changes drastically at the superionic phase transition, the problem of prime interest to us is that of analysing the temperature behaviour of the static conductivity coefficients. The calculated conductivity $\sigma(T)$ is represented in figure 2. One can see that at $\tau = \tau_{si}$ ($\tau_{si} = kT_{si}/|a|$), σ strongly increases, which is related to the change of the activation energy (see the insets of figure 2). Examination of the expressions (14) and (18) reveals that several different activation energies exist in the system in principle, which correspond to the contributions of the different transfer processes (the polaron hopping between different sublattices (H bonds) f or the intra-bond transfer within one sublattice f), and appear in the expression for the conductivity with different weight prefactors which in turn vary with temperature. The activation energy for the polaron intra-bond hopping is given by

$$E_a^T \sim \frac{1}{3}E_T^{ab} \pm \frac{1}{2}\hbar\Omega_{f,l} - (\tilde{\tau}_T^{ab})^2(\Omega_{f,l})^2 \tag{23}$$

whereas the activation energies for the inter-bond orientational hopping have the forms

$$\begin{aligned} E_a^{R(s)} &\sim \frac{5}{6}E_R^s \pm \frac{1}{2}(\gamma_{fs} - \gamma_{f's}) - (\tilde{\tau}_R^s)^2(\gamma_{fs} - \gamma_{f's})^2 \\ E_a^{R(ab)} &\sim \frac{1}{3}E_R^{ab} \pm \frac{1}{2}(-2\Omega_T + \gamma_{fb} - \gamma_{f'a}) - (\tilde{\tau}_R^{ab})^2(-2\Omega_T + \gamma_{fb} - \gamma_{f'a})^2. \end{aligned} \tag{24}$$

We see that the expressions (23) and (24) consist of the polaronic part (the first terms) and the parts which appear as a result of the transfer process, inter-proton interactions and proton orderings. Clearly, the activation energies should increase due to the second and third terms for $\tau < \tau_{si}$ when the proton ordering occurs in the system. We conclude from the insets of figure 2 that the activation energies in the superionic phases are actually lower that those in the ordered phases. It is apparent also that the drastic increase of σ obtained from (14) and (18) is significantly sharper as compared to the results obtained using the one-minimum approximation of the H-bond potential [6], when the inter-bond proton hopping process was neglected.

The increasing proton–phonon coupling parameters ∇V and $\nabla\Omega_T$ induce a decrease of σ due to the stronger localization of the proton within the H bond (see the dependences $\sigma(T)$

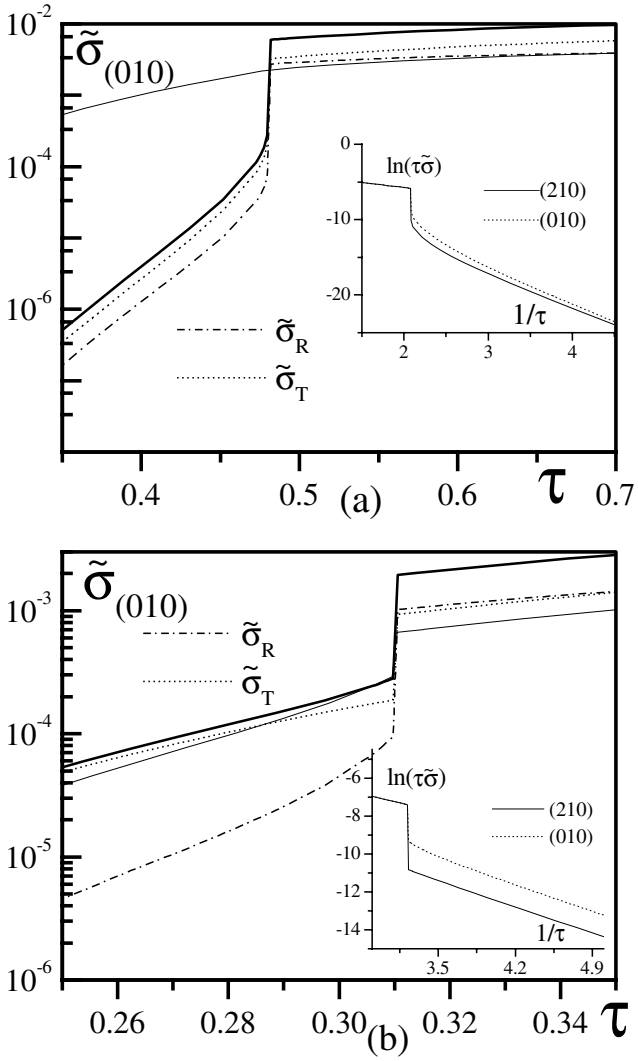

Figure 2. Temperature dependencies of the static protonic conductivity $\tilde{\sigma} = \sigma/c_0$ (bold solid line) ($c_0 = e^2\sqrt{\pi}a_0^2/\hbar v_c$) and its intra-bond and inter-bond hopping parts for $\omega_T = 0.05$, $\omega_R = 0.3$, $E_T^{ab}/|a| = 0.2$, $E_0/|a| = 1.0$. (a) $\tilde{b} = b/|a| = 1$ (the first-order superionic phase transition to the ordered state with the phase IV (TAHSe) proton ordering type) and (b) $\tilde{b} = 1.73$ (the first-order superionic phase transition to the ordered state with the phase III (TAHSe) proton ordering type). The curves denoted by thin solid lines correspond to the one-minimum H-bond approximation [6]; insets: the conductivity on a logarithmic scale along different directions.

plotted in figure 3(a) for different values of E_0 and E_T^{ab}). It also becomes apparent from figure 3 that the intra-bond dynamics strongly influences the magnitude of σ and the jump $\Delta\sigma$ at $\tau = \tau_{si}$. The increase of Ω_T and $|\nabla\Omega_T|$ leads to a lowering of σ and a decrease of $\Delta\sigma$. This effect is caused by the fact that the intensification of the intra-bond proton dynamics gives rise to the tendency of loss of the proton 'sensitivity' to the surroundings. We emphasize also that σ_R also drops with increasing Ω_T (see σ_R for different E_T^{ab} in the inset of figure 3(a)). The increase of Ω_T occurs due to the shortening of the O–O distance between H-bonded oxygens

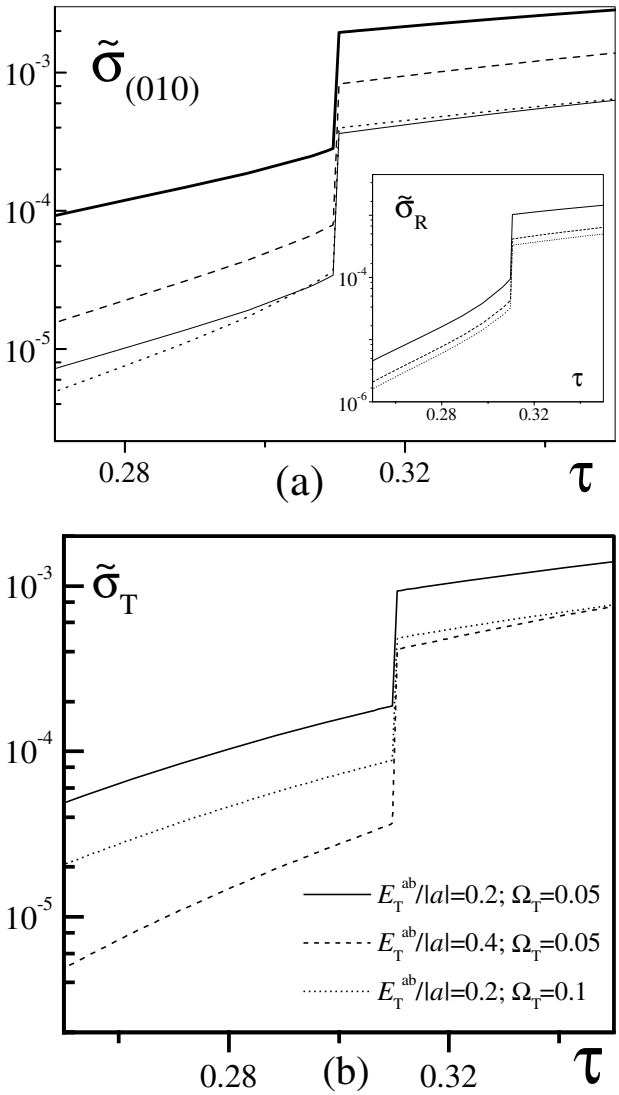

Figure 3. (a) The temperature dependence of σ for $\tilde{b} = 1.73$; the bold and thin solid curves correspond to the cases of $E_T^{ab}/|a| = 0.2$, $\omega_T = 0.05$, $\omega_R = 0.3$; $E_0/|a| = 1.0$ and $E_0/|a| = 1.5$ respectively. The dashed and dotted curves indicate the cases where $E_T^{ab}/|a| = 0.4$, $E_0/|a| = 1.0$, $\omega_R = 0.3$; $\omega_T = 0.05$ and $\omega_T = 0.3$ respectively. (b) The temperature dependence of the intra-bond contribution σ_T for $\tilde{b} = 1.73$, $\omega_R = 0.3$ and $E_0/|a| = 1.0$.

and the consequent strengthening of the H bond [19]. Therefore, more effort would be needed to break the H bond in comparison to the case for smaller Ω_T, and this is the reason for the decrease of the orientational inter-bond contribution σ_R. The decrease of Ω_T leads also to larger values of the phonon-assisted transfer part σ_T (see figure 3(b)). On the one hand, the fact that there is increase of σ with decrease of Ω_T is at variance with the well known results concerning the decrease of the conductivity upon D $\rightarrow$ H substitution. However, on the other hand, the substitution of D for H should induce an increase of the activation energy and, as a result, larger values of the polaronic binding energies E_0 and E_T^{ab} required to provide hopping

of a protonic polaron between two H bonds, and between two localized positions within the H bond respectively. The latter effect causes the conductivity to decrease as shown in figure 3.

Figure 4 shows the comparison of the theoretical conductivity obtained for TAHSe with the experimentally measured values [10] as well as with the result obtained using the previous one-minimum approximation [6]. The values of ∇V and $\nabla\Omega_T$ can be found from the dependences of the proton potential and tunnelling splitting energy on the distance between the oxygen ions evaluated in [19, 20]: in this case, $\nabla V \simeq 2.4$ eV Å^{-1} and $\nabla\Omega_T \simeq -0.5$ eV Å^{-1}. The two-stage approach gives us a significantly higher drastic increase of σ as compared to the results of [6]. We see that the conductivity coefficient is in better agreement with experiment [10] as compared to the results of reference [6], especially in the temperature region $\tau < \tau_{si}$. However, the jump $\Delta\sigma$ is sharper than that measured experimentally. It is interesting also that the contributions of the inter-bond and intra-bond processes differ strongly in different phases (see the inset of figure 4). The σ_R- and σ_T-contributions are of the same order in the superionic phase, whereas in the low-temperature ordered phases the reorientational hopping term σ_R is dominant and the intra-bond phonon-activated transfer is of lesser importance. Since, as we see, the discrepancies between experiment and theoretical results still remain after applying the more sophisticated two-stage treatment of proton transport incorporating the intra-bond transfer, let us analyse the activation energies for the conductivity in detail. It is known from [10] that the activation energy for the conductivity increases strongly from ∼0.32 eV in the superionic phase to ∼0.8 eV in the ordered phases. Although the activation energies (23) and (24) evaluated on the basis of (14) and (18) give a good agreement with experiment in the superionic state (∼0.37 eV), in the ordered states we have still lower values for E_a (∼0.45 eV). The one-minimum approximation [6] gives us ∼0.4 eV for $\tau < \tau_{si}$. Indeed, now that we have performed the analysis of both of the terms σ_R and σ_T, we understand that,

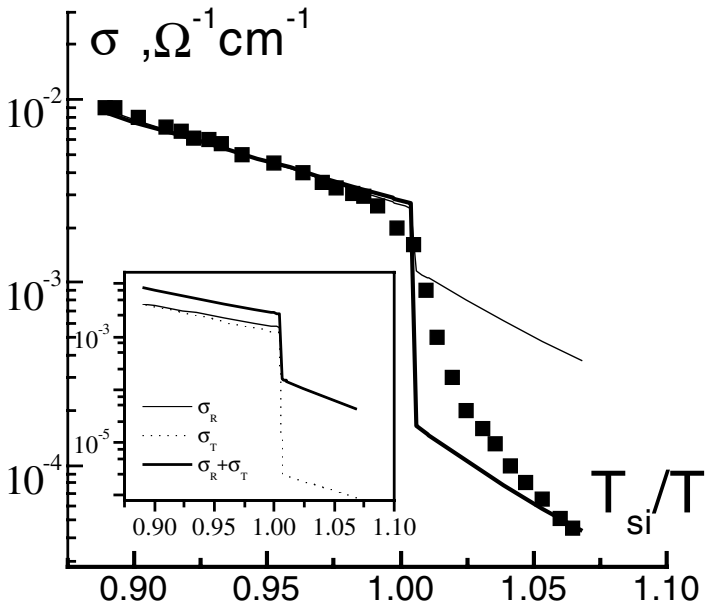

Figure 4. Comparison of the temperature dependences of the protonic conductivity, measured for the crystal TAHSe [10] (■), evaluated theoretically (bold curve) (in this case of $\Omega_T = 70$ cm^{-1}, $\Omega_R = 175$ cm^{-1}, $\hbar\omega_0 = 455$ cm^{-1}) and obtained using the one-minimum H-bond approximation [6] (thin curve).

since the contribution of σ_R at $\tau < \tau_{si}$ is predominant, the inclusion of intra-bond hopping makes just a small correction to σ in this temperature region, as is clear from the inset of figure 4. Therefore, the question that arises is: what other additional subtle reason can there be for the increase of E_a in the ordered state? The terms (24), giving in fact the activation energies at $\tau < \tau_{si}$, contain two essentially different parts. The part arising due to the inter-proton interactions changes only slightly on using a better approximation (using for instance the GFA [6] instead of the mean-field approach). Thus, the main reason for the change of E_a can only be the first terms in expressions (24) proportional to the polaron binding energies. Since the difference between experimental and theoretical values of E_a is about 0.35 eV, we can conclude that the polaron binding energies should increase by ∼0.42 eV (see E_R^s in (24)) in the low-temperature phases, reflecting the drastic increase of the polaron effective mass [21]

$$m^* \sim m \exp\left[\frac{5E_0}{3\hbar\omega_0}\right] \exp\left[\frac{5E_T^{ab}}{12\hbar\omega_0}\right]$$

(m is the bare proton mass), and consequently strengthening the localization of the proton between nearest oxygen ions. This additional transition between the state with weaker proton–phonon coupling at $\tau > \tau_{si}$ (smaller polaron mass) and the state with stronger coupling at $\tau < \tau_{si}$ (large polaron mass) has rather discontinuous character (with the jump of the polaron mass $\Delta m \sim \exp[5\Delta E_a/3\hbar\omega_0]$, $\Delta E_a \sim 0.42$ eV) and resembles the small-to-large-polaron transition occurring with a change of coupling to a certain phonon mode [22, 23] studied extensively for electron–phonon systems. Therefore, we can suggest that the redistribution of the proton at the transition between the superionic and ordered states must have a more complicated character incorporating at least two steps. First, with the temperature increasing, the polaron binding energy drops sharply due to the decrease of the effective proton–lattice distortion coupling. Second, the proton becomes redistributed between three possible H bonds in the unit cell with equal probability. In principle, the temperatures of the two stages could be different, which is a subject for further more sophisticated analysis. We just note here that for $Rb_3D(SO_4)_2$ crystal, NMR experiments [24] have detected deuteron inter-bond motion as a precursor of superionic conductivity already at 170 K below the superionic transition. Moreover, the latest scanning calorimetric measurements [11] show instead of the previously assumed single jump of the entropy $\Delta S = R \ln 3$ at $\tau = \tau_{si}$, a step-like increase of the entropy already at ∼1.5 K below the transition to the superionic state with only the total entropy change found to be $R \ln 3$. These results, exhibiting the sequential step-like redistribution of protons in the H-bonded network, support our conclusion. Further, to study comprehensively the temperature for the possible transition between the large- and smaller-polaron regimes, a more complicated scheme has to be used, incorporating the additional order parameter $\Delta\tau$ describing the change of proton–phonon coupling energy.

4. Summary

In conclusion, it is worth noting that the two-stage proton-transport mechanism introduced allows us to describe both the intra-bond and inter-bond contributions to the conductivity. The expression for the conductivity is derived using the Kubo theory for the regime of strong coupling between protons and anti-phase vibrational modes of the oxygen ions involved in the H-bond formation, which leads to the shortening of this bond and to the strong quasi-polaronic effect. The large energies of interaction between the protons and the oxygen distortions induce a significant decrease of the conductivity values due to proton localization within the H bond. The comparison with experiment makes it possible to draw several important conclusions. First, the inter-bond hopping process makes the main contribution to σ at $\tau < \tau_{si}$. Second, it

appears that the transition to the superionic state has a more complicated character involving a possible intermediate transition between the ordered state with a completely frozen-in H-bonded system and the superionic state with the protons redistributed between virtual H bonds with equal probability. The mechanism of this additional transition exhibiting a drastic change of the effective interaction between the protons and nearest O(2)-oxygen ions is a subject for further more sophisticated theoretical analysis.

References

[1] Belushkin A V, Carlile C J and Shuvalov L A 1995 *Ferroelectrics* **167** 21
[2] Yamada Y 1995 *Ferroelectrics* **170** 23
[3] Pavlenko N 2000 *Phys. Rev.* B **61** 4988
[4] Pavlenko N 2000 *J. Chem. Phys.* **112** 8637
[5] Stasyuk I V and Pavlenko N 1998 *J. Phys.: Condens. Matter* **10** 7079
[6] Pavlenko N 1999 *J. Phys.: Condens. Matter* **11** 5099
[7] Stasyuk I V, Pavlenko N and Hilczer B 1997 *Phase Transitions* **62** 135
[8] Stasyuk I V, Pavlenko N and Hilczer B 1998 *J. Korean. Phys. Soc* **32** S24
[9] Kreuer K D 1996 *Chem. Mater.* **8** 610
[10] Pawlowski A, Pawlaczyk Cz and Hilczer B 1990 *Solid State Ion.* **44** 17
[11] Kirpichnikova L, Hilczer B, Polomska M, Szczesniak L and Pawlowski A 2001 *Solid State Ion.* at press
[12] Pietraszko A, Hilczer B and Pawlowski A 1999 *Solid State Ion.* **119** 281
[13] Merinov B V, Bolotina N B, Baranov A I and Shuvalov L A 1980 *Crystallografiya* **33** 1387
[14] Merinov B V, Baranov A I and Shuvalov L A 1990 *Crystallografiya* **35** 355
[15] Merinov B V, Antipin M Yu, Baranov A I, Tregubchenko A M, Shuvalov L A and Struchko Yu T 1991 *Crystallografiya* **36** 872
[16] Kubo R 1957 *J. Phys. Soc. Japan* **12** 570
[17] Reik H G and Heese D 1967 *J. Phys. Chem. Solids* **28** 581
[18] Münch W, Kreuer K D, Traub U and Maier J 1995 *Solid State Ion.* **77** 10
[19] Scheiner S 1992 *Proton Transfer in Hydrogen-Bonded Systems* ed T Bountis (New York: Plenum)
[20] Maćkowiak M 1989 *J. Mol. Struct.* **192** 189
[21] Firsov Yu A (ed) 1975 *Polarons* (Moscow: Nauka) (in Russian)
[22] Toyozawa Yu 1961 *Prog. Theor. Phys.* **26** 29
[23] Das A N and Sil S 1993 *J. Phys.: Condens. Matter* **5** 8265
[24] Dolinšek J, Mikac U, Javoršek J E, Lahajnar C, Blinc R and Kirpichnikova L F 1998 *Phys. Rev.* B **58** 8445